APRIL 1983 LRP 221/83

TWO-MODE OPTICAL PUMPING OF A LASER

M.A. Dupertuis, R.R.E. Salomaa, M.R. Siegrist

TWO-MODE OPTICAL PUMPING OF A LASER

M.A. Dupertuis, R.R.E. Salomaa*, M.R. Siegrist

Centre de Recherches en Physique des Plasmas

Ecole Polytechnique Fédérale de Lausanne

Association Suisse - Euratom

CH 1007 Lausanne - Switzerland

* Helsinki University of Technology

Department of Technical Physics

SF-02150 Espoo 15

Finland

ABSTRACT

The coherent optical pumping of a laser is investigated by means of semi-classical laser theory with the assumption that either the pump source or the laser output is multimode. All radiation modes are allowed to reach saturating levels. A multitude of interesting effects results from induced population pulsations.

As a particular application we study numerically the optical pumping of a single mode homogeneously broadened FIR laser with a two-mode pump. We find that at least for symmetric pumping higher FIR intensities can be obtained with two, instead of one, pump modes.

I INTRODUCTION

Pulsed optically pumped high power FIR lasers are currently developed in several laboratories for plasma diagnostic purposes. The spectrum of FIR radiation collectively scattered from a tokamak-like plasma contains information on several important plasma parameters such as the ion temperature, impurity concentration and the magnetic field. The shape of the spectrally broadened laser line has to be analysed to extract the desired information. In the case of an initial laser line of width comparable to the scattered spectrum it is, in principle, possible to determine the effect of the plasma by deconvolution. In practice, however, it is necessary to select a laser of a bandwidth considerably smaller than the scattered spectrum. This is dictated by the very small cross-section of Thomson scattering and the associated difficulty of suppressing stray light. The spectrum of collectively scattered radiation from a typical tokamak plasma has a halfwidth of 1 to 2 GHz. This has to be compared with the mode spacing of the FIR laser on the order of 100 MHz. Clearly a single mode laser is required to fulfill the above condition.

So far the method applied to achieve single-mode FIR operation has been to pump the FIR laser with a single-mode CO_2 pulse. Several methods have been developed and successfully applied to achieve single-mode operation of a CO_2 laser. Most of them suffer from one great drawback: the efficiency of the oscillator and often the first amplifier is reduced considerably by mode discrimination. This is not an important consideration in a large system with several amplifying

stages. Due to the homogeneous broadening of the CO_2 gain line the total extracted energy in the power amplifiers under fully saturated conditions is almost independent of the mode structure. This is not the case in a small system where the low level single mode intensity produced by the oscillator is insufficient to saturate the amplifier along its whole length.

The motivation for the investigation reported in this paper is to establish conditions under which multimode pumping of a FIR laser can have a greater overall efficiency than single-mode pumping. FIR output is assumed to be single mode in both cases. The mathematical complexity of the general multimode problem is, however, quite formidable. We therefore have restricted our investigations to a proof of principle by treating only the case of a two-mode pump laser where both the pump and the FIR intensities are allowed to reach saturating levels.

We have found that the overall efficiency of two-mode pumping can indeed exceed the single mode efficiency under certain conditions which will be discussed in section 3.

In section 2 we outline the theoretical treatment based on the density matrix formalism. The population densities are obtained in terms of matrix continued fractions. In section 3 we present and analyse the results of numerical computations. Experimental implications, mainly in connection with the FIR laser resonator, are discussed in section 4 which is followed by some concluding remarks.

II THEORY

We have applied Lamb's [1] laser theory to describe the interaction of a three-level molecular system (neglecting degeneracies) with two laser fields and a thermal bath. Only recently it has been discovered [2,3] that two-photon Raman type effects are important in optically-pumped FIR lasers. The theory presented here will connect Panock and Temkin's work [3] with multimode theories of systems involving only two levels. Mathematically analogous problems arise in the context of double optical resonance and radiofrequency spectroscopy performed with standing wave lasers [4 - 9].

The method of solution is outlined for a general case where both the FIR and pump fields may be multimode and have arbitrary intensities. A more detailed analysis is restricted to a special situation where the pump consists of two modes and the FIR output is single mode. Although of limited applicability, this approach yields interesting general information on the multimode pumping of FIR lasers and can, at the expense of increased complexity, be extended to more complicated configurations.

The classical field is composed of discrete pump and FIR modes. For simplicity we choose travelling waves according to

$$E(z,t) = \frac{1}{2} \sum_n E_n \exp\left[i (K_n z - \Omega_n t) \right] + c.c.$$
$$\mathcal{E}(z,t) = \frac{1}{2} \sum_m \mathcal{E}_m \exp\left[i (k_m z - \nu_m t) \right] + c.c. \qquad (1)$$

where E represents the optical pump field and ε the FIR laser field. The active medium consisting of molecules is described in terms of an idealized three level model shown in Fig. 1. The polarization induced by the fields is calculated with the standard density matrix formalism [10] which is only briefly outlined below. The density matrix $\tilde{\rho}$ obeys the master equation

$$i\hbar\,\dot{\tilde{\rho}} = [H, \tilde{\rho}] + i\hbar \left.\frac{\delta\tilde{\rho}}{\delta t}\right|_{rel} \tag{2}$$

where $\dot{\tilde{\rho}}$ represents the convective derivative $(\partial_t + v\,\partial_z)\tilde{\rho}$ (v is the velocity of the molecule along the laser axis z) and $\delta\tilde{\rho}/\delta t|_{rel}$ includes incoherent pumping and relaxation of the levels. The Hamiltonian contains the unperturbed part H_0 and the dipole interaction term $\bar{\mu} \cdot (\bar{E} + \bar{\varepsilon})$.

With the rotating wave approximation we are allowed to assume that the amplitudes

$$\begin{aligned}
\rho_{21} &= \tilde{\rho}_{21}\, \exp\left[-i\,(Kz - \Omega t)\right] \\
\rho_{23} &= \tilde{\rho}_{23}\, \exp\left[-i\,(kz - \nu t)\right] \\
\rho_{31} &= \tilde{\rho}_{31}\, \exp\left[-i\left((K-k)z - (\Omega-\nu)t\right)\right] \\
\rho_{ii} &= \tilde{\rho}_{ii}
\end{aligned} \tag{3}$$

vary slowly compared to the combination frequencies $\Omega_n + \Omega_m$, $\nu_n + \nu_m$, and $\Omega_n + \nu_m$. For the central frequencies and corresponding wavenumbers (K, Ω) and (k, ν) we can pick one of the pairs appearing in (1). Inserting (1) and (3) into (2) we find

$$
\begin{aligned}
\dot{\rho}_{11} &= \Gamma_1 (\mathring{n}_1 - \rho_{11}) + 2\ \mathrm{Im}\,(\alpha^* \rho_{21}) \\
\dot{\rho}_{22} &= \Gamma_2 (\mathring{n}_2 - \rho_{22}) - 2\ \mathrm{Im}\,(\alpha^* \rho_{21} + \beta^* \rho_{23}) \\
\dot{\rho}_{33} &= \Gamma_3 (\mathring{n}_3 - \rho_{33}) + 2\ \mathrm{Im}\,(\beta^* \rho_{23}) \\
\dot{\rho}_{21} &= -(\gamma_{21} + i\,\Delta_{21})\,\rho_{21} + i\,\alpha\,(\rho_{22} - \rho_{11}) - i\,\beta\,\rho_{31} \\
\dot{\rho}_{23} &= -(\gamma_{23} + i\,\Delta_{23})\,\rho_{23} + i\,\beta\,(\rho_{22} - \rho_{33}) - i\,\alpha\,\rho_{31}^* \\
\dot{\rho}_{31} &= -(\gamma_{31} + i\,\Delta_{31})\,\rho_{31} + i\,\alpha\,\rho_{23}^* - i\,\beta^*\rho_{21}
\end{aligned}
\tag{4}
$$

where $\Gamma_i(n_i^0 - \rho_{ii})$ and $-\gamma_{ij}\rho_{ij}$ are relaxation terms, the detunings are denoted by

$$
\begin{aligned}
\Delta_{21} &= \omega_{21} - \Omega + Kv \\
\Delta_{23} &= \omega_{23} - \nu \\
\Delta_{31} &= \Delta_{21} - \Delta_{23} = \omega_{31} - \Omega + \nu + Kv
\end{aligned}
\tag{5}
$$

and the Rabi flipping parameters by

$$
\begin{aligned}
\alpha &= \frac{1}{2\hbar}\,\mu_{21} \sum_n E_n \exp\left[i\,(K_n - K)z - i\,(\Omega_n - \Omega)\,t\right] \\
\beta &= \frac{1}{2\hbar}\,\mu_{23} \sum_m \mathcal{E}_m \exp\left[-i\,(\nu_m - \nu)\,t\right]
\end{aligned}
\tag{6}
$$

In (5) and (6) we have neglected the Doppler shift of the FIR transition; similarly we can ignore the spatial dependence in (6) for corunning pump modes since usually the residual Doppler shift $|K_n - K|v$ is very small (note that in a standing wave case this simplification is not generally allowed).

Let us assume that we have N equidistant pump modes, i.e.

$$\Omega_{n+1} = \Omega_1 + n\delta \qquad (n = 0, \ldots, N-1) \tag{7}$$

and a single mode FIR field oscillating at the frequency ν_1. The flipping frequencies (6) reduce to

$$\alpha = \sum_{p=0}^{N-1} \alpha_{p+1} \exp(-ip\delta t) \quad ; \quad \beta = \beta_1 \tag{8}$$

where $\alpha_p = \mu_{21} E_p / 2\hbar$ and $\beta_1 = \mu_{23}\ \varepsilon_1 / 2\hbar$. Assuming that α_p and β_1 do not vary within γ^{-1} we obtain a stationary solution of eqs. (4) as a Fourier series

$$\rho_{ij}(t) = \sum_{m=-\infty}^{+\infty} \rho_{ij}(m) \exp(-im\delta t) \tag{9}$$

where the components $\rho_{ij}(m)$ satisfy the recursion relations

$$\begin{aligned}
\rho_{11}(m) &= L_1(m)\Gamma_1 \mathring{n}_1 \delta_{m,0} - iL_1(m)\left[\sum_p \alpha^*_{p+1}\rho_{21}(m+p) - \alpha_{p+1}\rho^*_{21}(-m+p)\right] \\
\rho_{22}(m) &= L_2(m)\Gamma_2 \mathring{n}_2 \delta_{m,0} + iL_2(m)\left\{\left[\sum_p \alpha^*_{p+1}\rho_{21}(m+p) - \alpha_{p+1}\rho^*_{21}(-m+p)\right] + \beta^*\rho_{23}(m) - \beta\,\rho^*_{23}(-m)\right\} \\
\rho_{33}(m) &= L_3(m)\Gamma_3 \mathring{n}_3 \delta_{m,0} - iL_3(m)\left[\beta^*\rho_{23}(m) - \beta\,\rho^*_{23}(-m)\right] \\
\rho_{21}(m) &= i\ell_{21}(m)\left[\sum_p \alpha_{p+1}\left(\rho_{22}(m-p) - \rho_{11}(m-p)\right) - \beta\,\rho_{31}(m)\right] \\
\rho_{23}(m) &= i\ell_{23}(m)\left[\beta\left(\rho_{22}(m) - \rho_{33}(m)\right) - \sum_p \alpha_{p+1}\rho^*_{31}(-m+p)\right] \\
\rho_{31}(m) &= i\ell_{31}(m)\left[\sum_p \alpha_{p+1}\rho^*_{23}(-m+p) - \beta^*\rho_{21}(m)\right]
\end{aligned} \tag{10}$$

with the complex Lorentzian factors

$$L_j(m) = (\Gamma_j - im\delta)^{-1} \quad ; \quad \ell_{jk}(m) = \left[\gamma_{jk} + i(\Delta_{jk} - m\delta)\right]^{-1} \tag{11}$$

This (infinite) linear system of equations has to be solved for the unknowns $\rho_{ij}(m)$.

The assumption of a single mode FIR field leads to equations involving one-dimensional Fourier series (9) only. No additional complications arise if we assume that the FIR field has the same periodicity as the pump, i.e.

$$\beta = \sum_{k=0}^{M-1} \beta_{k+1} \exp(-ik\delta t) \tag{12}$$

or if the pump is single mode and in (12) we use the FIR mode spacing $\delta_{FIR} = \nu_{m+1} - \nu_m$ for δ. In the case when both the pump is multimode and several FIR cavity eigenmodes are present simultaneously eqs. (4) lead to two-dimensional Fourier series

$$\rho_{ij}(t) = \sum_{m,n} \rho_{ij}(m,n) \exp\left[-i(m\delta + n\delta_{FIR})\, t\right] \tag{13}$$

which is much more laborious to solve than eq. (10).

The polarization of the medium is given by $\mathrm{Tr}\{\vec{\mu}\rho\}$. With the aid of (3) and (9) we obtain for the polarization at the FIR frequency

$$\rho_{FIR} = -\sum_{m} \mu_{23}\, \beta_{23}(m) \exp(-im\delta t) \exp[i(kz - \nu t)] + c.c \tag{14}$$

Inserting this into the Maxwell equations in which we make the slowly varying envelope approximation and integrate over the beat period δ^{-1} we find for the FIR intensity

$$\frac{d}{dt}|\mathcal{E}_1|^2 = G_{FIR,1}\,|\mathcal{E}_1|^2 \tag{15}$$

where the gain is given by

$$G_{FIR,1} = \frac{2\nu\mu_{23}}{\varepsilon_0 c}\,\mathrm{Im}\left(\frac{\rho_{23}(0)}{\mathcal{E}_1}\right) \tag{16}$$

Equation (14) contains also beat notes ($m \neq 0$) which act as a drive for new FIR modes separated from the original one by a multiple of δ. A comparison with (12) reveals that the corresponding gain for the FIR mode m is given by

$$G_{FIR,m} = \frac{2\nu\mu_{23}}{\varepsilon_0 c}\,\mathrm{Im}\left(\frac{\rho_{23}(m-1)}{\mathcal{E}_m}\right) \tag{17}$$

When solving for ρ_{23} (m) the presence of several FIR modes has to be taken into account by using the generalised form of (10). A separate summation of FIR mode indices is necessary, too. In the following we assume that only β_1 is present. We also simplify the parameter analysis by choosing equal relaxation rates $\gamma = \Gamma_i = \gamma_{ij}$.

Our numerical code solves eqs. (10) with matrix continued fractions and Gauss elimination. The code reproduces exactly the single mode results reported by Panock and Temkin [3] as well as results which were obtained by a simpler numerical approach based on a continued fraction treatment of the strongly coupled transition 1↔2, but restricting the FIR intensity to the small signal regime. We have

tested for symmetries and verified also that phases are not important in this particular context. Details of the calculational method are given in the Appendix.

It is worthwhile noting that our treatment can easily be applied to a range of different schemes. Specifically, in Doppler broadened systems, the two counterpropagating parts of a single-mode standing wave, each interacting resonantly with a different set of molecules, can be interpreted as two separate modes of a travelling wave [11]. With the same code cascade configurations, saturation effects in double resonance spectroscopy as also different pump and resonator systems of optically-pumped cw-FIR lasers can be described. Some of these schemes are schematically shown in Fig. 2.

III NUMERICAL RESULTS

In order to present our results in system-independent units, we introduce a normalised dimensionless spatial growth parameter defined by

$$g = |\tilde{\beta}| \; \mathrm{Im}\left(\frac{\tilde{\rho}_{12}}{\tilde{\beta}\,\tilde{n}_1}\right) \tag{18}$$

where we have removed the phase factor and normalised with respect to the equilibrium population n_1^0 of the ground level. The field strengths α and β as well as the intermode spacing δ and the detunings Δ_{jk} are also made dimensionless by defining

$$\tilde{\alpha} = \frac{\alpha}{\gamma} \; ; \; \tilde{\beta} = \frac{\beta}{\gamma} \; ; \; \tilde{\delta} = \frac{\delta}{\gamma} \; ; \; \tilde{\Delta}_{jk} = \frac{\Delta_{jk}}{\gamma} \qquad (19)$$

where γ is the relaxation rate of the levels, assumed to be the same for all levels. The FIR intensity gain can now be written

$$G_{FIR} = \frac{\nu \mu_{23}^2 \hat{n}_4}{\hbar \varepsilon_0 c \gamma} \frac{g}{\tilde{\beta}} \qquad (20)$$

and hence is proportional to g for a constant field amplitude $\tilde{\beta}$.

In Fig. 3 we show calculated profiles of the spatial growth parameter g for a range of different operating conditions. The four curves in each graph represent the following arrangements of pump modes: (1) one pump mode on line center, (2) one pump mode offset from line center by four Lorentzian line widths, (3) symmetric pumping with two modes mutually separated by eight Lorentzian line widths and (4) asymmetric two-mode pumping with one mode on line center and the second one again offset by eight Lorentzian line widths.

The figure is grouped into three columns of three graphs, according to the saturation parameters $\tilde{\alpha}$ and $\tilde{\beta}$ for the pump and the FIR, respectively. From top to bottom the pump intensity grows from a small signal via a saturating level to a strongly saturated case and the same applies to the FIR intensity, going from left to right.

In the top left graph we notice that for small pump and FIR signals a high gain can only be obtained by resonant pumping. The gain

profiles due to the resonant single mode pump and the asymmetric two mode pump with one mode on line center are practically identical. The off-resonant mode only contributes a small bump at its Raman shifted frequency. The center-line gain for these two cases is considerably higher than for the two off-resonant cases (2) and (3). For weak pump intensities the total gain profile is just a superposition of the gain profiles of the two separate pump modes. Since one off-resonant mode in this regime results in two gain peaks of equal height, one on line center and one at the Raman line, the result of pumping with two symmetric modes is a profile with three peaks, one at each of the two respective Raman lines and one, twice as high, on line center.

Since the conditions discussed are prevalent at an early stage in the pump pulse which is critical for the build-up of the FIR pulse, it follows that the mode structure of the pump mode has a very important influence on the development of the FIR pulse.

If the pump intensity is now increased (2nd and 3rd graph of first column) we notice that the ratio of the gains due to off-resonant and resonant pumping becomes more favorable for off-resonant pumping. This is due to the fact that saturation is reached more rapidly with resonant pumping. For $\tilde{\alpha} = 1$ just barely visible and for $\tilde{\alpha} = 5$ fully developed is the effect of AC Stark splitting of the gain line. Since the FIR mode structure is fully developed by the time this condition is reached, Rabi-splitting is undesirable since it shifts the gain peak away from the position of the FIR mode. The structure due to Rabi splitting is considerably more complicated for

the multimode cases. Multiple peaks are observed with a separation which reflects the intermode spacing. This is due to nonlinear effects resulting from the induced beating of the population densities. Part of this structure can be explained using a dressed atom formalism [12]. The small signal FIR gain is generally lower and broader with multimode pumping.

Moving from left to right in the figure corresponds to increasing the FIR power. Hereby the top right and center graphs do not correspond to a very realistic case in the context of FIR lasers: saturated FIR intensities at small signal pump intensities. Due to power broadening the detailed structure observed in the small-signal regime is smeared out at high FIR intensities.

In a FIR oscillator, as in any laser oscillator which is pumped long enough to reach steady-state conditions, the FIR intensity will grow up to a point where the gain is reduced by saturation to a value which just equals the averaged round trip losses. Significant saturation is only reached for $\tilde{\beta} > 1$. This indicates that the bottom two graphs in the rightmost column probably best represent the desirable operating conditions. While the parameter to be optimised is the FIR intensity exiting from the oscillator, which is not related to the gain in a simple way, we can nevertheless conclude that similar FIR intensities will result from comparable gain values. The gain values obtained for the conditions of Figs 3 f and i are indeed quite similar, but the pump power necessary to achieve this is $\tilde{\alpha}^2 = 25$ times higher in the bottom graph. Guided by the figure one would obviously choose to operate the laser with the parameters according to Fig. 3 f.

If we compare the different pump mode distributions in this figure, assuming that the FIR mode has developed on line center, we notice immediately that pumping with two symmetrical modes around the line center yields the best result. The gain (Fig. 3 f) drops to about 60 % if one of these modes is suppressed, whereas strong saturation results from pumping on line center with one mode. For asymmetric two-mode pumping the gain is high, but offset from line center.

At much higher pump intensities (Fig. 3 i) the differences between the various pump schemes almost disappear.

Fig. 3 clearly demonstrates that the optimisation of an optically pumped FIR laser is not an easy task. Gain profiles are sensitive functions of pump and FIR intensities both of which vary continuously during the pulse. While the small signal behaviour is easily predictable, many high intensity effects are not yet well understood. Especially one can anticipate a rather complicated behaviour when several pump and FIR modes are simultaneously present. A much more detailed analysis is obviously required. Some encouragement for this is provided by our main result that in an interesting operation range two-mode pumping can be an advantage.

IV FIR RESONATOR CONSIDERATIONS

In order to derive the operating point of a FIR oscillator we represent the data corresponding to the right hand side of Fig. 3 in a

different way and include the effect of the oscillator cavity, neglecting spatial effects (radial profiles, pump depletion and FIR gain along the axis) and dispersion. For the same four arrangements of pump modes we show in Fig. 4 the normalised density matrix element as a function of $\tilde{\beta}$. Since g according to eq. 20 is proportional to the gain times the field amplitude ε (or $\tilde{\beta}$) the cavity loss curve in this representation appears as a straight line through the origin with a slope proportional to the averaged cavity roundtrip loss. The operating point of the active resonator is the cross-over point of this line with one of the curves, that is

$$g = \frac{c}{Q}\,\tilde{\beta} \qquad ; \qquad C = \frac{\ell\,\varepsilon_0\,\gamma^2}{\mu_{23}^2\,\dot{n}_1} \tag{21}$$

where Q is the quality factor of the cavity and C a constant. The cavity loss curve shown in Fig. 4 (Q = 40000, C = 41.4) corresponds to a 4 m long D_2O-laser resonator at a wavelength of 385 μm with overall roundtrip losses of 25 % and a reflectivity of the output coupler of 5 %.

For this particular resonator we can now see from Fig. 4 that the FIR intensity obtained with symmetric two mode pumping is approximately twice as high as with resonant single mode pumping. It has to be remarked, however, that the total pump energy is also twice as high in the first case, since we assumed $\tilde{\alpha} = 1$ for each pump mode. To allow for a comparison of single mode and two mode pumping for a constant total pump mode energy, we have included in Fig. 4 also a curve representing single mode pumping with $\tilde{\alpha} = \sqrt{2}$. We find that at least for the resonator chosen the obtainable FIR energy is practically the same for

single mode pumping and symmetric two-mode pumping. This suggests that at least from the point of view of reproducibility of the FIR output careful mode control of the pump source is not necessarily required. The importance of this statement lies in the fact that mode selecting elements in the cavity usually entail considerable losses.

We have made an investigation similar to the one presented in Fig. 3 for two off-resonant pump modes separated from the line center by 16 and 24 linewidths and compared the results to single mode pumping at detunings 16, 20 and 24 linewidths from the line center. Since higher pump and FIR intensities are necessary to saturate a Raman transition we have calculated gain spectra for all combinations of $\tilde{\alpha}$, $\tilde{\beta}$ = 0.01, 1, 5, 10, 15. The results indicate that in this case two mode pumping is not very attractive.

We find that in the small signal regime (i.e. $\tilde{\alpha}$, $\tilde{\beta} \ll \tilde{\delta}$, $|\tilde{\Delta}_{21}|$) the total gain is simply a superposition of the two individual gain contributions (see Fig. 5 a). Since the two Raman frequencies are different one obtains two separate gain peaks, one at each Raman frequency. Both pump modes also produce a gain peak of equal height on line center. Their superposition is a gain peak of twice the height which, at a first glance, looks attractive. However, to operate an off-resonantly pumped FIR laser on line center is very inefficient, since the line center gain saturates much more rapidly than the Raman gain. For $\tilde{\alpha} = \tilde{\beta} = 1$ the combined gain on line center has already dropped to half of the Raman gain of a single mode pump at the mid-frequency of the two modes considered (Fig. 5 b). For $\tilde{\beta} = 5$ the gain on line center is no longer visible on the graph (Fig. 5 c).

At a stage where the intensities are so large that the two broadened Raman gain lines overlap significantly enough to make two mode pumping attractive, the position of the gain peak is shifted by a considerable amount. Since the frequency of the FIR mode which developes in the resonator is fixed, the increased gain at a shifted frequency is useless. This should be contrasted with the symmetric pumping where the lineshifts are opposite and cancel for $\tilde{\alpha}_1 = \tilde{\alpha}_2 = \tilde{\alpha}$. We conclude from this investigation that off-resonant two-mode pumping could only be advantageous in very specific operating conditions.

An interesting case, especially from the theoretical point of view, is shown in Fig. 6. For the pump frequencies indicated above we display the small signal gain profiles for strongly saturating pump modes. Under these conditions the ac Stark effect is very important. The line center gain peak is shifted towards negative frequencies, approximately by the same amount for all three single mode cases considered and considerably more for the two-mode case (with twice the total energy). The Raman lines are also shifted, but in the opposite direction. Apart from these shifts the single mode gain profile is not greatly affected. Specifically it still contains two peaks only: the on-line and the Raman gain peaks. This changes considerably with two mode pumping. Due to the population pulsation effects discussed earlier, additional gain peaks at the intermode frequencies appear. The intermode frequency for the case shown is 8 and the average separation of the peaks 8.2. Theoretically two combs of peaks with a separation of the mode distance δ should appear in the limit $\gamma \to 0$ [12].

A situation like the one shown is realised experimentally when a FIR cavity with a relatively long buildup time is pumped with a rapidly rising pump pulse. When the pump pulse has already reached its maximum power, the FIR pulse is still in the buildup phase and hence sees this complicated modulated gain profile. Obviously there is now a strong tendency that multiple FIR modes develop with a mode separation that reflects the cavity roundtrip time of the pump laser resonator. The following two qualitative observations which support this idea have been made in our experiments: (a) with multimode pumping mode beating with a beat frequency corresponding to the pump laser cavity can be obtained in a low-quality FIR resonator or a superradiant tube, (b) if the pump pulse is not perfectly tuned to a single mode, single mode FIR radiation is obtained more readily with a gently rising pump pulse.

V CONCLUSIONS

In this paper we have investigated optical pumping of a FIR resonator with the assumption that either the pump source or the FIR output is multimode. The general theory has been outlined and discussed. The following simplifying assumptions in the model used have to be considered when the theory is applied to describe an experimental situation: (i) the degeneracy of the energy levels has been ignored, (ii) collisions are only treated in terms of relaxation rates, (iii) optical transitions such as cascade and refill transitions are ignored. However, in the treatment presented, all radiation modes are

allowed to reach saturating levels, resulting in a multitude of interesting effects.

A particular application is then investigated numerically: The optical pumping of a single mode laser with a pump source consisting of two modes. Certain effects have again been neglected to reduce the complexity: (i) all relaxation rates considered are assumed to be equal, (ii) spatial variations in a resonator are neglected (iii), at equilibrium only the lower level is populated, and (iv) no Doppler broadening is considered.

We find that at least for symmetric pumping higher FIR intensities can be obtained with two-mode pumping. The reason for this is (i) that no line splitting occurs due to the pump radiation (the splittings due to the two symmetric modes cancel) and (ii) pump saturation is rather weak because both modes are off-resonant. If this can really be turned into a great advantage in a experimental situation depends on the ease with which a multimode pumped FIR laser can be forced to emit a single mode only. Alternatively, single mode operation of the FIR laser may not always be required. This, however, represents a new, more complicated situation. Since extrapolations from the current model calculations are not readily applicable, investigations of this kind are planned for a future publication.

APPENDIX

In this appendix we outline a method to solve the infinite system of linear equations (10). We then discuss the relative merits of using matrix continued fractions over other methods.

To reduce the number of unknowns in (10) we substitute the diagonal elements and the last equation for $\rho_{31}(m)$ in the two equations involving $\rho_{21}(m)$ and $\rho_{32}(m)$. This yields

$$
\begin{aligned}
\rho_{21}(m) = {} & i\, l_{21}(m)\, \alpha_{m+1}\, \dot{r}_{21}\, \chi_E(m) \\
& - l_{21}(m) \Big\{ \sum_{p\in E} \alpha_{p+1} L_2(m-p) \left[\beta^* \rho_{23}(m-p) - \beta\, \rho_{23}^*(-m+p)\right] + \\
& + \sum_{p\in F} \left[\sum_{q\in E} \alpha_{p+q+1} \left(L_2(m-p-q) + L_1(m-p-q)\right) \alpha_{q+1}^* \right] \rho_{21}(m-p) - \\
& - \sum_{p\in G} \left[\sum_{q\in E} \alpha_{p-q+1} \left(L_2(m-p+q) + L_1(m-p+q)\right) \alpha_{q+1} \right] \rho_{21}^*(-m+p) \Big\} \\
& - l_{21}(m)\, \beta\, l_{31}(m) \left[\beta^* \rho_{21}(m) - \sum_{p\in E} \alpha_{p+1} \rho_{23}^*(-m+p) \right]
\end{aligned}
\tag{A 1}
$$

$$
\begin{aligned}
\rho_{23}(m) = {} & i\, l_{23}(m)\, \beta\, \dot{r}_{23}\, \delta_{m,0} \\
& - l_{23}(m)\, \beta \Big\{ L_2(m) \left[\sum_{p\in E} \alpha_{p+1}^* \rho_{21}(m+p) - \alpha_{p+1} \rho_{21}^*(-m+p) \right] + \\
& + \left(L_2(m) + L_3(m)\right) \left[\beta^* \rho_{23}(m) - \beta\, \rho_{23}^*(-m) \right] \Big\} \\
& - l_{23}(m) \Big\{ \sum_{p\in F} \left[\sum_{q\in E} \alpha_{p+q+1}\, l_{31}^*(-m+p+q)\, \alpha_{q+1}^* \right] \rho_{23}(m-p) - \\
& - \sum_{p\in E} \alpha_{p+1}\, l_{31}^*(-m+p)\, \beta\, \rho_{21}^*(-m+p) \Big\}
\end{aligned}
$$

where

$$E = \{0, \ldots, N-1\} \; ; \; F = E \ominus E \; ; \; G = E \oplus E \; ; \text{ and } \alpha_{m+1} = 0 \text{ if } m \notin E$$

with $\chi_E(m) = 1$ if $m \in E$

$\chi_E(m) = 0$ otherwise

In these two infinite sets of linear complex algebraic equations for $\rho_{21}(m)$ and $\rho_{23}(m)$ there are only a few inhomogeneous terms for $m \in E$. The system has a unique solution with the property $\rho_{21}(m)$, $\rho_{23}(m) \to 0$ when $m \to \pm \infty$. A proof can be found in Bambini [13, 14] for a problem of a similar nature. We define a set of complex 2 x 2 matrices and vectors such that (A1) can be written as

$$\sum_{\rho \in F} \underline{\underline{a}}(m,\rho)\ \underline{x}(m-\rho) + \sum_{\rho \in G} \underline{\underline{b}}(m,\rho)\ \underline{y}(m-\rho) = \underline{c}\ \chi_E(m) \qquad \text{(A2)}$$

where

$$\underline{x}(m) = \begin{pmatrix} \rho_{21}(m) \\ \rho_{23}(m) \end{pmatrix} \quad \text{and} \quad \underline{y}(m) = \underline{x}^*(-m) \quad \text{for } m \in \mathbb{Z} \qquad \text{(A3)}$$

We now restrict ourselves to the case of a two-mode pump where $E = \{0, 1\}$. For $|m| < 2$ (A2) is an under-determined linear system (UDLS) of 10 equations and 16 complex unknowns.

For $m > 2$ (A3) gives:

$$\underline{\underline{a}}(m,1)\ \underline{x}(m-1) + \underline{\underline{a}}(m,0)\ \underline{x}(m) + \underline{\underline{a}}(m,-1)\ \underline{x}(m+1) +$$

$$+ \underline{\underline{b}}(m,2)\ \underline{y}(m-2) + \underline{\underline{b}}(m,1)\ \underline{y}(m-1) + \underline{\underline{b}}(m,0)\ \underline{y}(m) = 0$$

Taking the complex conjugate of (A2) written for $-m$ where $m > 2$ we get the independent equation :

$$\underline{\underline{a}}^*(-m,1)\ \underline{x}^*(-m-1) + \underline{\underline{a}}^*(-m,0)\ \underline{x}^*(-m) + \underline{\underline{a}}^*(-m,-1)\ \underline{x}^*(-m+1) +$$

$$+ \underline{\underline{b}}^*(-m,2)\ \underline{y}^*(-m-2) + \underline{\underline{b}}^*(-m,1)\ \underline{y}^*(-m-1) + \underline{\underline{b}}^*(-m,0)\ \underline{y}^*(-m) = 0$$

For convenience we define a set of complex 4 x 4 matrices $\underline{\underline{A}}(m)$, $\underline{\underline{B}}(m)$, $\underline{\underline{C}}(m)$, $\underline{\underline{D}}(m)$, $\underline{\underline{E}}(m)$ such that using (A3) the last two equations can be written as

$$\underline{\underline{A}}(m)\,\underline{X}(m-2) + \underline{\underline{B}}(m)\,\underline{X}(m-1) + \underline{\underline{C}}(m)\,\underline{X}(m) + \underline{\underline{D}}(m)\,\underline{X}(m+1) + \underline{\underline{E}}(m)\,\underline{X}(m+2) = 0$$

$$\text{where} \quad \underline{X}(m) = \begin{pmatrix} x(m) \\ y(m) \end{pmatrix} \qquad \text{and} \quad m > 2 \tag{A4}$$

This five term recurrence relation can be solved by continued fractions with the following ansatz :

$$\underline{\underline{R}}(m)\,\underline{X}(m-2) + \underline{\underline{S}}(m)\,\underline{X}(m-1) = \underline{X}(m) \quad \text{for } m > 2 \tag{A5}$$

We replace $\underline{X}(m + 1)$ and $\underline{X}(m + 2)$ in (A4) by (A5) written for $\underline{X}(m + 1)$ and $X(m + 2)$ and factorise the coefficients of $\underline{X}(m - 2)$ and $\underline{X}(m - 1)$. The results can be compared with equation (A5) which yields the following iteration formula :

$$\begin{aligned} \underline{\underline{R}}(m) &= -\,\underline{\underline{U}}(m)\,\underline{\underline{A}}(m) \\ \underline{\underline{S}}(m) &= -\,\underline{\underline{U}}(m)\left[\underline{\underline{B}}(m) + \underline{\underline{V}}(m)\,\underline{\underline{R}}(m+1)\right] \end{aligned} \tag{A6}$$

where

$$\underline{\underline{U}}(m) = \left[\underline{\underline{C}}(m) + \underline{\underline{V}}(m)\,\underline{\underline{S}}(m+1) + \underline{\underline{E}}(m)\,\underline{\underline{R}}(m+2)\right]^{-1}$$

$$\underline{\underline{V}}(m) = \underline{\underline{D}}(m) + \underline{\underline{E}}(m)\,\underline{\underline{S}}(m+2)$$

Using the fact that all elements of $\underline{\underline{A}}$, $\underline{\underline{B}}$, $\underline{\underline{C}}$, $\underline{\underline{D}}$, $\underline{\underline{E}}(m)$ are either zero or of the order of $1/m^2$ (except the elements of the diagonal of $\underline{\underline{C}}(m)$ which are of the order of 1) it is easy to show that all elements of

$\underline{\underline{R}}$ and $\underline{\underline{S}}(m)$ are of the order of $1/m^2$. This is consistent with the requirement that $\lim_{m\to\infty} \underline{X}(m)$ should be zero for a physical solution.

If we now assume that $\underline{\underline{R}}(K+1)$, $\underline{\underline{R}}(K+2)$, $\underline{\underline{S}}(K+1)$, $\underline{\underline{S}}(K+2) = 0$ for a sufficiently large K it is easy to see that the relative error of each element of $\underline{\underline{R}}(K)$, $\underline{\underline{S}}(K)$, $\underline{\underline{R}}(K-1)$, $\underline{\underline{S}}(K-1)$, ... obtained from (A6) will be of the order of $1/K^2$, $1/K^4$, ... hence decreasing rapidly towards negligible values. K has to be chosen large enough that the matrices $\underline{\underline{R}}(4)$, $\underline{\underline{S}}(4)$, $\underline{\underline{R}}(3)$, $\underline{\underline{S}}(3)$ resulting from the iterative process (A6) do not change by more than 10^{-4} to 10^{-6} when the process is repeated with a higher number of iteration steps.

Together with the UDLS the equations

$$\begin{aligned} \underline{\underline{R}}(3)\,\underline{X}(1) + \underline{\underline{S}}(3)\,\underline{X}(2) &= \underline{X}(3) \\ \underline{\underline{R}}(4)\,\underline{X}(2) + \underline{\underline{S}}(4)\,\underline{X}(3) &= \underline{X}(4) \end{aligned} \qquad \text{(A7)}$$

form a system of 18 complex equations with 18 unknows, having a unique solution. If we construct $\underline{X}(m)$ with (A5) $\lim_{m\to\infty} \underline{X}(m) = 0$, and hence this is the unique solution of (A1) and (A2). The final system is solved by Gauss elimination to obtain $\rho_{21}(0)$, $\rho_{21}(-1)$ and $\rho_{23}(0)$.

Further generalisation of our continued fraction solution to treat the multimode case where $\mathbf{E} = \{0, 1, \ldots, N-1\}$, and involving only 4 x 4 matrices (cf ref 15), is possible. However, the iteration formula (A6) and the final system become significantly more complicated. For a constant truncation order K the computer time increases as N^2.

Our generalisation of continued fractions to solve the five-term recurrence relation (A4) is always convergent because the form of the continued fractions have been carefully adapted to the order of the coefficients in the recurrence relation. We have to point out that this is not the case for the previous generalisation proposed by Hambenne and Sargent [11]. The lack of convergence of their solution is apparent in their eq. 69 (HB69). From (HB57) and (HB52) we see that c_{jk} is of the order of $1/k$ for $j \neq 0$ and of the order of k for $j = 0$. If one starts from (HB69) with some high order value of k and sets $r_{k+i} = 0$ for $i > 0$, r_k will be of the order of 1, r_{k-1} of the order of $1/k^2$, r_{k-2} of the order of 1, etc. However, the computed r_1 are no longer similar if the starting order is changed to $k + 1$. The source of the problem lies in the error propagation. Although equation (HB69) is mathematically correct, the initial 100 % error is not attenuated but propagated since the largest coefficient in the denominator is the coefficient of r_{1+1}.

An alternative numerical method to solve equation (10) is to transform the system formed by the UDLS and (A4) into a real linear system $\underline{\underline{A}}\ \underline{V} = \underline{b}$ truncated at some high order K where $\underline{\underline{A}}$ is a band matrix of a total width of 25 elements and $\underline{V}$ a vector composed alternatively by the real and imaginary parts of $\underline{x}(0)$, $\underline{x}(1)$, $\underline{y}(1)$, $\underline{x}(2)$, etc. Let us now compare the direct and iterative methods [16] to solve this system with our matrix continued fractions.

We will first make some comments on the more obvious case of a three-term scalar recurrence relation involving the usual continued

fractions [17]. This algorithm may be thought of as a particular case of the Thomas algorithm [18] which is known to be the most efficient method to treat linear tridiagonal systems on serial computers. As a consequence of the large number of zero-elements in the inhomogeneous term the efficiency is even higher. It is also possible to show that for high orders k negligible error propagation occurs [19,20] in continued fractions when off-diagonal elements are of the order k^{-2}. Moreover, according to Feldman and Feld [4] or Abramowitz and Stegun [17] it is possible to construct the solution of the system of order k + 1 from the solution of the system of order k with very few operations. This property should also be very useful for matrix continued fractions if the off-diagonal matrices are regular.

Coming back now to our specific problem, the situation is less clear. For direct as well as for iterative methods of solutions of the real system, the number of operations needed to obtain an approximate solution is proportional to the number of equations and to the square of the total width of the system. Using the same rule for our generalised continued fraction solution we found that for $k > 7$ continued fractions were more efficient, reaching a typical factor of 2.5 at $k = 100$ and 2.8 when $k \to \infty$. We attribute this to the use of complex arithmetics and the economy of the right-hand side computation in continued fractions (except in the final part of the calculation).

On the other hand, iterative methods offer the advantage to be able to increase the number of equations and choose the optimum K simultaneously with the iteration. Another way to increase efficiency

would be to take advantage of the fact that the coefficient matrices $\underline{\underline{A}}$, $\underline{\underline{B}}$, $\underline{\underline{C}}$, $\underline{\underline{D}}$, $\underline{\underline{E}}(m)$, as well as $\underline{\underline{R}}$, $\underline{\underline{S}}(m)$, contain a certain number of zeros. A more complicated recurrence relation could be found or a sparse matrix solver could be used [7,8]. However, the possibly resulting small advantage may not be worth the effort.

As a conclusion, when the inhomogeneous part of a linear system is zero except for a few nearly contiguous terms, continued fraction solutions appear to be an interesting alternative to the more commonly used methods.

References

[1] W.E. Lamb Jr., Phys. Rev. 134, A1429 (1964).

[2] S.J. Petuchowski, A.T. Rosenberger, and T.A. de Temple, IEEE J. of Quantum Electron. QE13, 476 (1977).

[3] R.L. Panock and R.J. Temkin, IEEE J. of Quantum Electron. QE13, 425 (1977).

[4] B.J. Feldman and M.S. Feld, Phys. Rev. A5, 899 (1972).

[5] M. Allegrini, E. Arimondo, and A. Bambini, Phys. Rev. A15, 718 (1977).

[6] E. Kyrölä and R. Salomaa, Phys. Rev. A23, 1874 (1981).

[7] A.H. Paxton and P.W. Milonni, Phys. Rev. A26, 1549 (1982)

[8] A.H. Paxton and P.W. Milonni, Opt. Commun. 34, 111 (1980).

[9] T. Oka, Frontiers in Laser Spectroscopy, vol. 2, Eds. R. Balian, S. Haroche and, S. Liberman, North-Holland, Amsterdam (1977), pp.531-569.

[10] M. Sargent III, M.O. Scully, and W.E. Lamb, Laser Physics, Addison Wesley, New York (1974).

[11] J.B. Hambenne, M. Sargent III, Phys., Rev. A13, 784 and 797 (1982).

[12] P.R. Berman, and R. Salomaa, Phys. Rev. A25, 2667 (1982).

[13] A. Bambini, Phys. Rev. A14, 1479 (1976).

[14] A. Bambini, Phys. Letts. 59A, 379 (1976).

[15] E. Arimondo and G. Moruzzi, J. Phys. B15, 73 (1982).

[16] L. Fox, "An Introduction to Numerical Linear Algebra", Clarendon Press, Oxford (1964).

[17] M. Abramowitz, and I.A. Stegun, "Handbook of Mathematical functions", Dover, New-York (1972), p.19, 9th edition.

[18] L.H. Thomas, Watson Sci. Comput. Lab. Rept., Columbia University, New York (1949).

[19] W.F. Ames, "Numerical methods for Partial Differential Equations", 2nd edition, Academic Press, New York (1977) p. 53.

[20] G.D. Smith, "Numerical solution of partial differential equations", 2nd edition, Clarendon Press, Oxford (1978) p.26.

Figure captions

Fig. 1 : The three-level, two-mode pump configuration used in this paper.

Fig. 2 : Equivalent configurations which can be treated with the two-mode code:

a) optically-pumped FIR laser with ring resonator (no standing wave).

b) double resonance spectroscopy in a resonator.

c) optically-pumped low-pressure laser

solid line: standing wave in Doppler broadened transition

broken line: travelling wave.

Fig. 3 : Spectral profiles of the spatial growth parameter g (prop. to the FIR gain) for different pump and FIR amplitudes $\tilde{\alpha}$ and $\tilde{\beta}$, respectively. Four different arrangements of pump modes are compared (see inset Fig. 3a). Horizontal axis (frequency) from $-20\tilde{\Delta}_{21}$ to $20\tilde{\Delta}_{21}$ in each graph. Vertical axis from zero to $N \cdot 10^{-6}$, where N is the number in the top left corner of each graph.

Fig. 4 : Spatial growth parameter g as function of FIR amplitude, for fixed pump amplitudes. Four pump mode arrangements are compared. The cavity loss curve appears as straight line. Its intersection with the curves gives the operating point of a FIR laser.

Fig. 5 : Spectral profiles of the spatial growth parameter q for off-resonant single and two-mode pumping

a) in the small signal regime the gain with two pump modes is a linear superposition of the two individual gain contributions.

b) and c) show the rapid saturation on line center.

Fig. 6 : As Fig. 5, but for saturating pump intensities. Gain peaks at intermode frequency spacing appear with two-mode pumping.

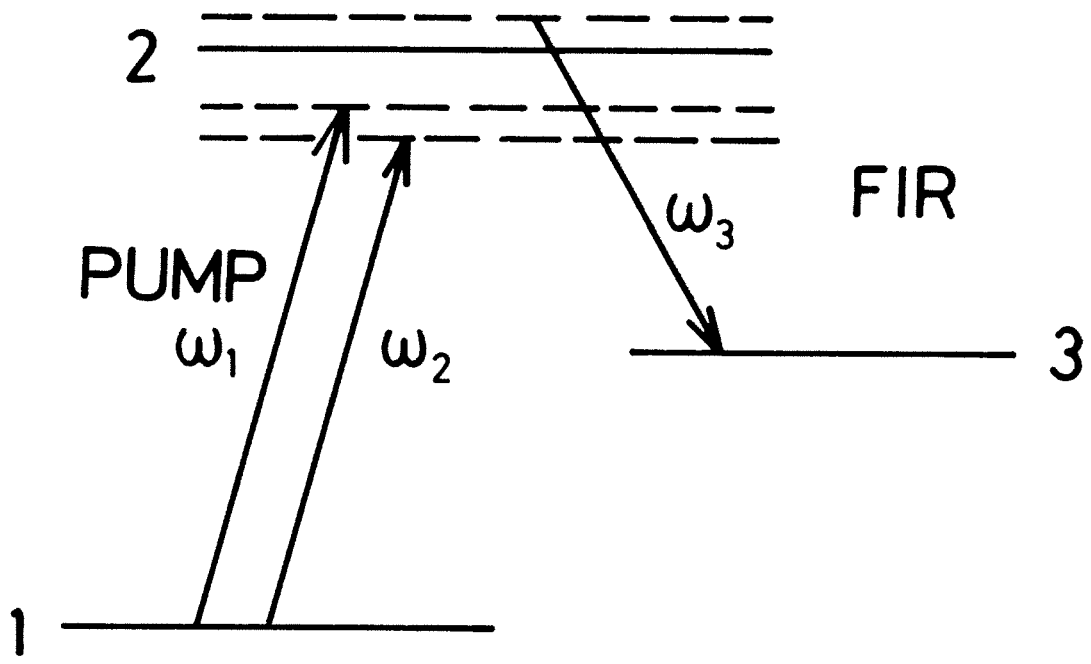

FIG. 1

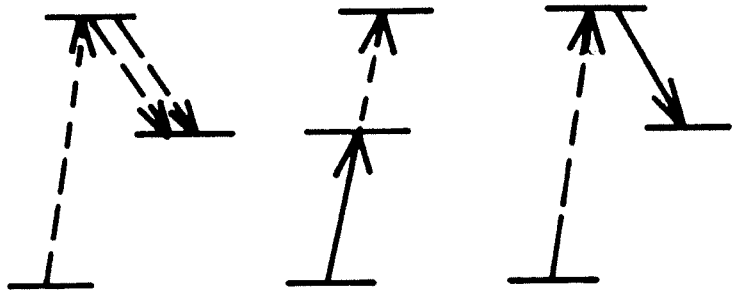

FIG. 2

FIG. 3

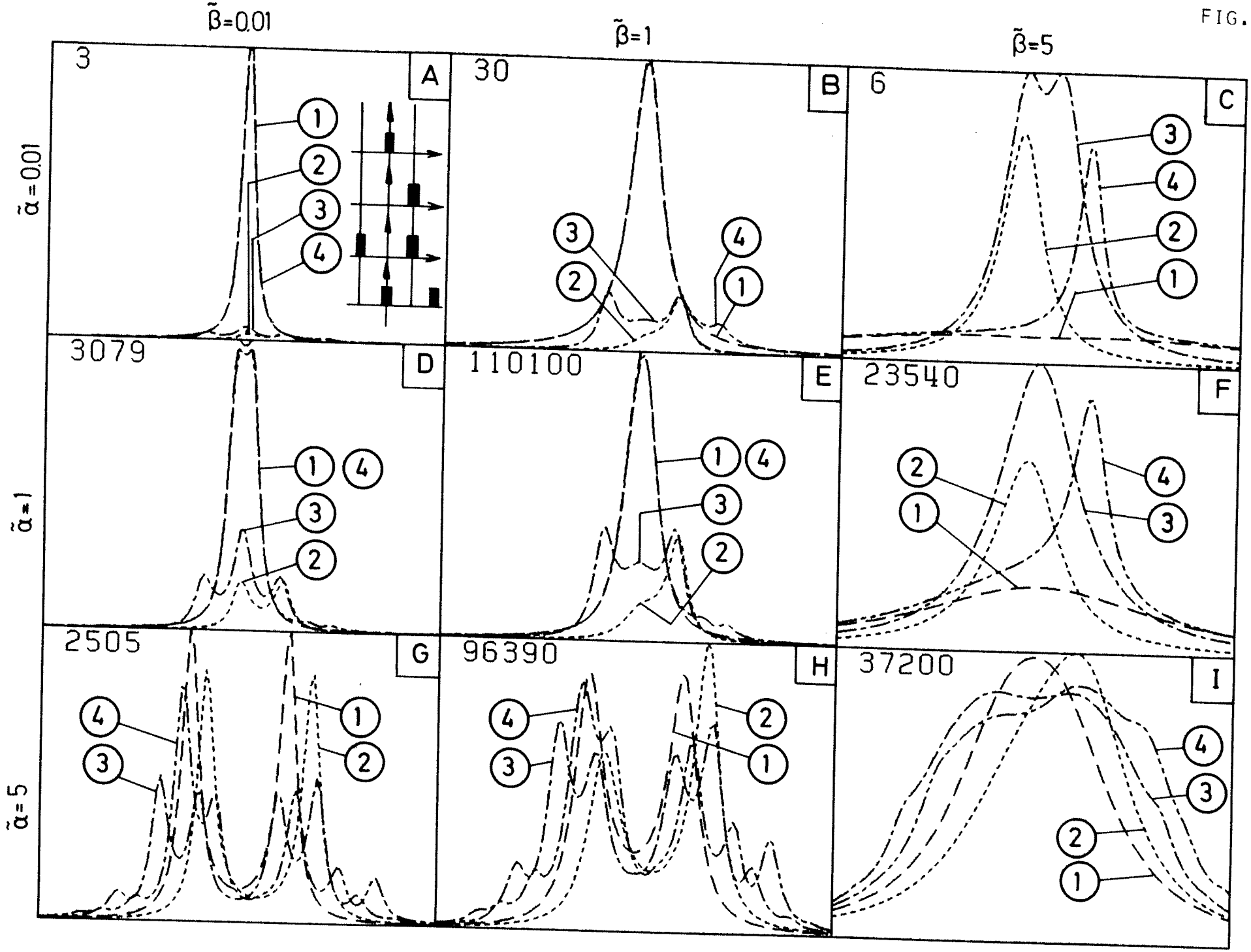
β̃=0.01
β̃=1
β̃=5
α̃=0.01
α̃=1
α̃=5
3
A
30
B
6
C
3079
D
110100
E
23540
F
2505
G
96390
H
37200
I

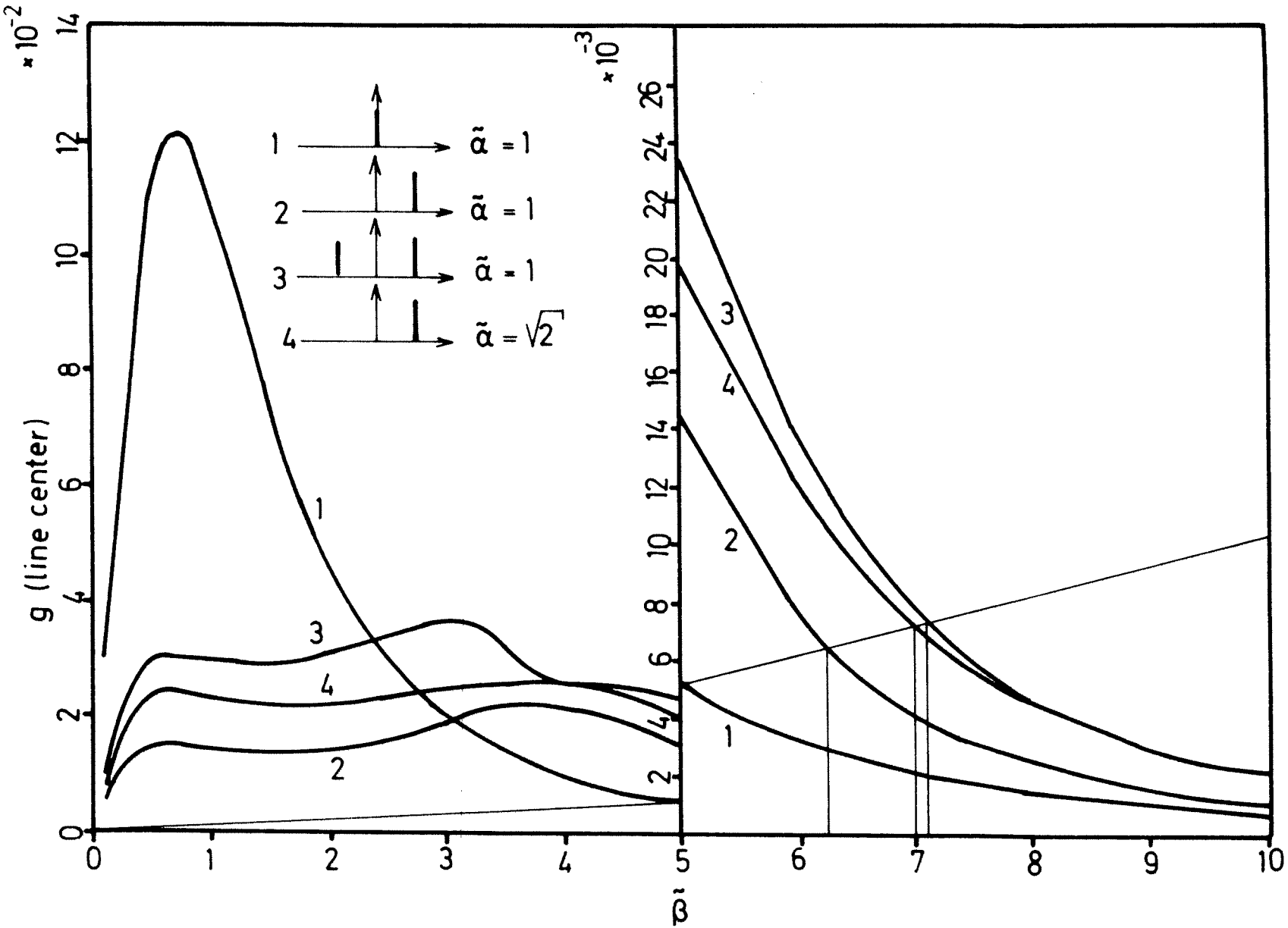

FIG. 4

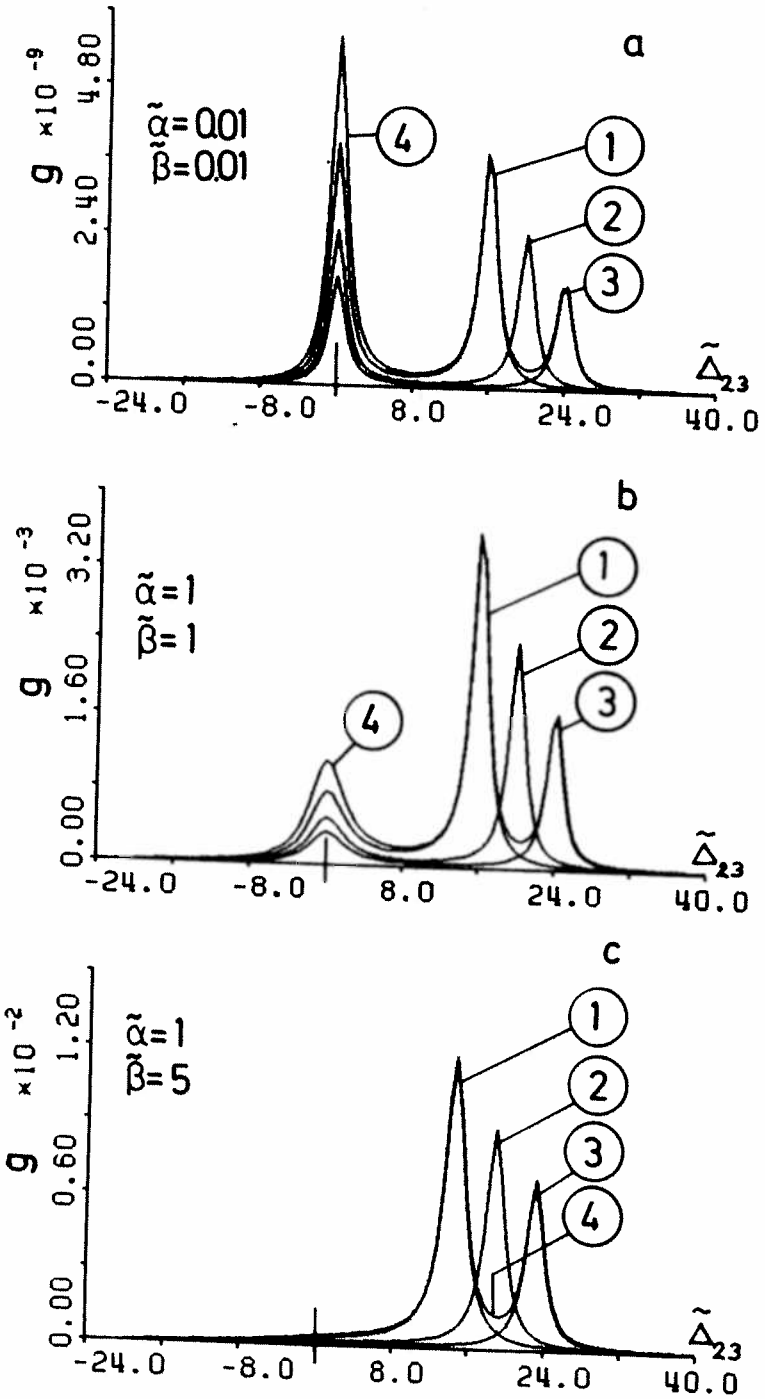
a
g ×10⁻⁹
4.80
2.40
0.00
α̃=0.01
β̃=0.01
1
2
3
4
Δ̃23
-24.0
-8.0
8.0
24.0
40.0
b
g ×10⁻³
3.20
1.60
0.00
α̃=1
β̃=1
1
2
3
4
Δ̃23
-24.0
-8.0
8.0
24.0
40.0
c
g ×10⁻²
1.20
0.60
0.00
α̃=1
β̃=5
1
2
3
4
Δ̃23
-24.0
-8.0
8.0
24.0
40.0

FIG. 5

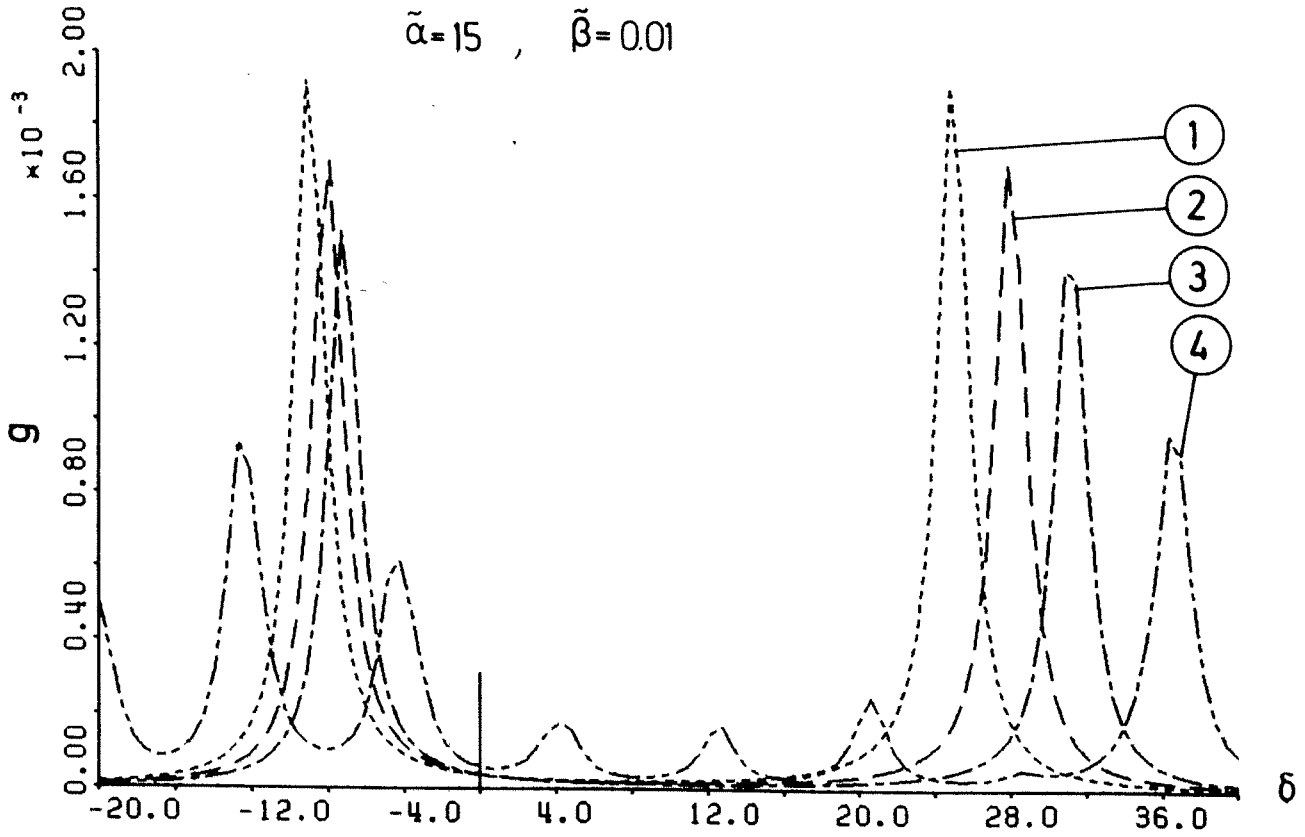
$\tilde{\alpha}$=15 , $\tilde{\beta}$=0.01
g
×10⁻³
0.00
0.40
0.80
1.20
1.60
2.00
-20.0
-12.0
-4.0
4.0
12.0
20.0
28.0
36.0
δ
1
2
3
4

FIG. 6